XX

Intramolecular Homolytic Substitutions in Synthesis

Sara H. Kyne and Carl H. Schiesser

School of Chemistry and Bio21 Molecular Science and Biotechnology Institute, The University of Melbourne, Victoria, Australia

1 INTRODUCTION

Free radical chemistry contributes to the modern chemists' toolbox in ways that were unimaginable only a few decades ago. There can be no doubt that the construction of carbocyclic and heterocyclic ring systems through the intramolecular addition of alkyl, aryl, and other radicals to unsaturated functionalities is a major contribution to synthetic methodology; this chemistry is the topic of other contributions to this collective work. It is important to recognize that the fundamental principles that guide the use of intramolecular homolytic addition chemistry in synthesis, eloquently summarized by Giese in his 1986 monograph,[1] also apply to intramolecular homolytic substitution chemistry. It was recognized some time ago that most organic free radical addition reactions are under kinetic control and this means that an understanding of fundamental rate and mechanistic data are crucial in designing useful chemical reactions based on these free radical processes[1]; the same holds true for reactions involving homolytic substitution chemistry.

Intramolecular homolytic substitution chemistry for the construction of heterocycles was in its infancy as recently as 20 years ago, having largely been used for constructing sulfur-containing ring systems. One of us contributed to a comprehensive review on homolytic substitution chemistry some 15 years ago,[2] and more recently, presented a feature article,[3] while other reviews have been written on the topic since then.[4,5] The purpose of this article is to provide a practical guide to intramolecular homolytic substitution chemistry, focusing primarily on chemistry developed over the past decade. It is intended to deliver a cross-section of information of relevance to the synthetic practitioner as well as to provide relevant experimental procedures. It is deliberately not meant to be comprehensive, but rather, through examples, intended to provide useful information about the state-of-play of radical substitution chemistry, and what is possible using this relatively new addition to the chemists' toolbox.

2 FUNDAMENTAL PRINCIPLES

To fully appreciate the scope and limitations of homolytic substitution processes at higher heteroatoms, one needs to appreciate the mechanisms by which these reactions proceed, and their associated rate constants. It has been generally agreed that three mechanisms exist for these reactions (Scheme 1).[2] These include a backside mechanism similar to S_N2, leading to Walden inversion, as well as a frontside mechanism that would result in retention of configuration at asymmetric heteroatoms such as silicon, germanium, or tin. The third possibility involves a hypervalent

Encyclopedia of Radicals in Chemistry, Biology and Materials. Edited by Chryssostomos Chatgilialoglu and Armido Studer.
 ISBN: 978-0-470-97125-3.

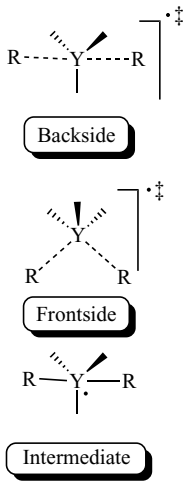

$R^{\bullet} + X{-}L \longrightarrow R{-}X + L^{\bullet}$

X	Inter-molecular	Intra-molecular
H	✔	✔
SiR_3	✔	✔
GeR_3	✔	✔
SnR_3	✔	✔
SR	✔	✘
SeR	✔	✘
TeR	✔	✘
Cl	✔	✘
Br	✔	✘
I	✔	✘

Scheme 1 Inter- versus intramolecular homolytic substitution at main group higher heteroatoms.

intermediate that may or may not undergo pseudorotation before dissociation, possibly resulting in racemization when the heteroatom undergoing attack is stereogenic.

Homolytic group (and atom) transfer reactions can involve either inter- or intramolecular homolytic substitution processes. Scheme 1 summarizes the trends observed for these reactions, and these trends provide useful information in relation to cyclization reactions at main group higher heteroatoms. The data provided in Scheme 1 indicate that intermolecular group transfer reactions have been reported for hydrogen, as well as for most of the main group elements. However, the analogous intramolecular process is only observed for hydrogen, silicon, germanium, and tin. To the best of our knowledge, there are no reported examples of intramolecular homolytic substitution at the pnictogens (N, P, As); however, several intermolecular examples exist.[6]

These observations raise obvious questions such as why do group 14 elements undergo this intramolecular chemistry while there are no reported examples for the chalcogens and halogens? Computational chemistry as well as carefully constructed experiments have shed light on the underlying reasons for the trends observed for these group transfer reactions.[7–12]

Other than the substitution at hydrogen, which would appear to "go around corners" because of the orbitals involved during homolytic substitution, for the remaining main group elements, the backside mechanism requires a collinear (or nearly so) arrangement of attacking and leaving radicals with deviations from this geometry resulting in unfavorable processes with high-energy transition states. For example, Wild showed that 1,4-, 1,5-, and 1,6-homolytic translocations of chlorine, bromine, and iodine have prohibitively high-energy barriers as determined by MP2/DZP calculations (Scheme 2) consistent with substantially "bent" transition state geometries at the halogen (120–145° for 1,5-translocations).[7] Wild also determined the angular dependence of the MP2/DZP calculated energy for the transition state (**1**) involved in the degenerate reaction of methyl radical with chloromethane. As the angle (θ) is reduced from 180° (ideal) there is a continual rise in transition state energy to a maximum at 90° at which point the transition state has suffered an increase in energy of about 112 kJ mol^{-1}.[7] While there was a 3.4 kJ mol^{-1} decrease in progressing to 80°, no saddle point for a frontside mechanism was located. It is clear from this study that homolytic substitution at halogen has a strong preference for backside attack in which the attacking and leaving radicals adopt a collinear arrangement.[7]

Similar observations are made for translocation reactions involving chalcogen. Computational studies suggest that group transfer processes

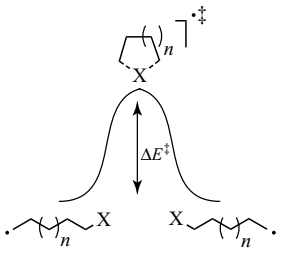

	$\Delta E^{\ddagger}$ (kJ mol^{-1})		
n	Cl	Br	I
2	191.0	—	—
3	170.9	149.2	136.0
4 (C_s)	163.5	137.9	120.0
4 (C_2)	198.4	175.6	—

MP2/DZP

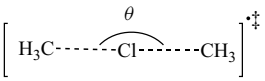

1

Scheme 2 Dependence of geometry on homolytic halogen translocation reactions.

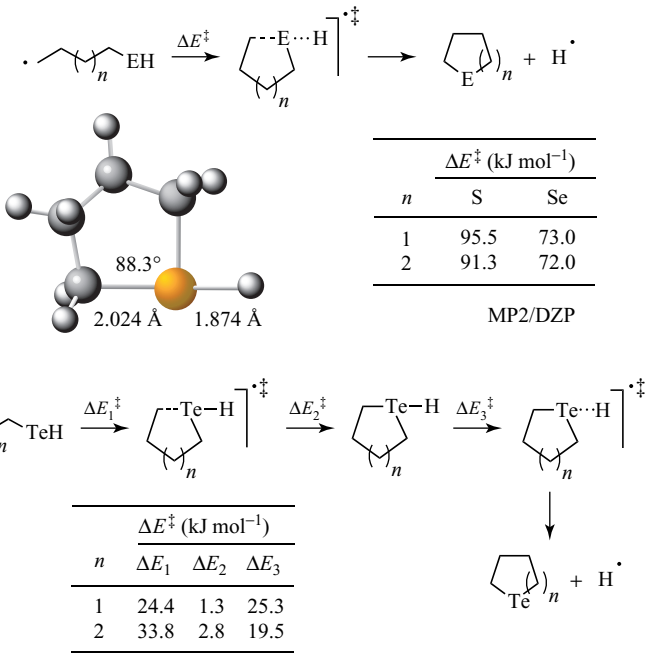

	$\Delta E^{\ddagger}$ (kJ mol^{-1})	
n	S	Se
1	95.5	73.0
2	91.3	72.0

MP2/DZP

	$\Delta E^{\ddagger}$ (kJ mol^{-1})		
n	ΔE_1	ΔE_2	ΔE_3
1	24.4	1.3	25.3
2	33.8	2.8	19.5

Scheme 3 Some calculated homolytic ring closures at sulfur, selenium, and tellurium.

involving homolytic substitution at sulfur and selenium proceed through a backside mechanism and, as was predicted for halogen, have prohibitively high energy barriers, once again the result of significant deviations from the ideal geometry for backside attack at these heteroatoms.[8] MP2/DZP calculations provide energy barriers in the 90–140 kJ mol^{-1} range for 1,5-, 1,6-, and 1,7-chalocogen transfer, depending on the heteroatom. However, unlike halogen, Wild was able to locate a second transition state for intramolecular homolytic substitution at sulfur and selenium, and that transition state led to the formation of the corresponding heterocycle.[8] Indeed, so unfavorable is intramolecular translocation at sulfur and selenium that even a hydrogen atom is calculated to prefer to leave, resulting in the formation of the heterocycle in preference to group transfer (Scheme 3)! So, here we have a fundamental difference between chalcogen and halogen: the second substituent on the chalcogen can act as a leaving group; indeed, it would appear to be easier to adopt the required "backside attack" orientation of attacking and leaving radicals during ring formation, than during translocation.

The story is slightly more complicated for reactions involving tellurium in that radical attack at tellurium mostly results in the formation of hypervalent intermediates; however, they are calculated to lie in very shallow wells on their respective potential energy surface and, as a consequence, behave in a similar manner to their sulfur and selenium counterparts in relation to the overall chemistry observed (Scheme 3).[8]

Given these computational data, one might begin to imagine ways of engineering systems that would result in efficient ring formation and it is no surprise that many synthetically useful examples of this chemistry are carried out using stable radical leaving groups such as *tert*-butyl and benzyl.

So, what about silicon, germanium, and tin? Computational and mechanistic studies have revealed that homolytic substitution at these heteroatoms can proceed by using either frontside or backside substitution mechanisms, with both pathways often in competition with each other.[9] For example, the degenerate reaction of silyl radical with disilane is calculated to have CCSD(T)/aug-cc-pVDZ//MP2/aug-cc-pVDZ energy barriers of 52.7 and 58.2 kJ mol^{-1} for the frontside and backside pathways, respectively (Scheme 4).[9] Similar results have been obtained for other systems.[10,13] Clearly, unlike the chalcogens

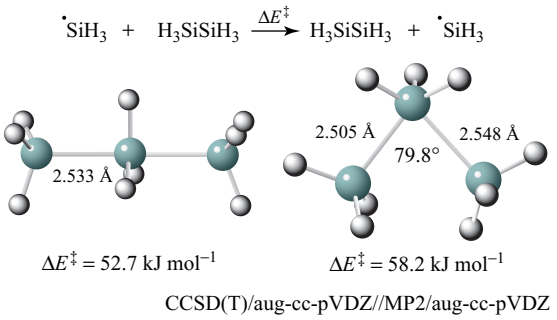

Scheme 4 Backside versus frontside mechanisms in the homolytic substitution of silyl radical at disilane.

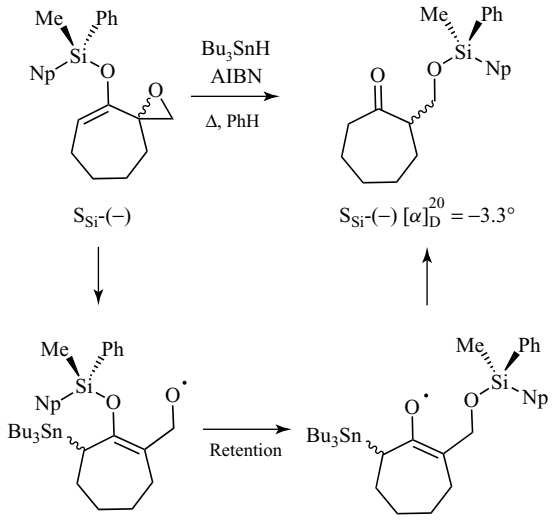

Scheme 5 Example of a 1,5-translocation involving an asymmetric silicon substituent.

and halogens, this chemistry at the group 14 higher heteroatoms does not require collinear arrangements of attacking and leaving radical, and the (approximately) 80° requirement for the frontside transition state is convenient for group transfer chemistry.

These computational studies were nicely complemented by the work of Horvat who showed that homolytic translocation involving a stereogenic silicon atom proceeds with retention of configuration, consistent with the involvement of a frontside transition state (Scheme 5).[11]

To summarize this section, homolytic substitution at the chalcogens and halogens proceeds via backside mechanisms that involve transition states in which the attacking and leaving radicals prefer to adopt a collinear (or nearly so) arrangement. This requirement introduces prohibitive amounts of strain in the transition states for 1,*n*-translocation reactions. However, it can be harnessed to generate chalcogen-containing ring systems that include molecules such as tetrahydroselenophene. In the case of elements such as silicon, germanium, and tin, this chemistry can proceed via frontside or backside mechanisms leading to translocation and cyclization possibilities. Examples of these chemistries are provided below.

3 INTRAMOLECULAR HOMOLYTIC SUBSTITUTION AT THE CHALCOGENS

3.1 Kinetic Data for Ring-Closure Reactions

Unlike intramolecular homolytic addition chemistry that abounds with useful rate data for the synthetic practitioner to use in crafting the optimum conditions for their reactions of interest (see **Radical Kinetics and Clocks**, Volume 1), fewer rate data are available for ring-closure reactions involving radical attack at higher heteroatoms. As mentioned earlier, because radical reactions are usually under kinetic control, the availability of rate constants for key (model) reactions is crucial for their success in the laboratory. For that reason, we have decided to include the available kinetic data for ring closure at sulfur, selenium, and tellurium in this article (Table 1). While most of the data for sulfur were reported in the 1996 review,[2] or in the more recent compilation by Crich,[5] rate constants for these reactions at selenium and tellurium have never been reported together before; their inclusion here provides valuable insight into intramolecular homolytic substitution involving these elements.

The data presented in Table 1 clearly show that rate constants for homolytic substitution at the chalcogens depend on three key factors: (i) the nature of the heteroatom, (ii) the size of the ring being formed, and (iii) the stability of the leaving group. Keeping ring size and leaving radical the same, in progressing down the group from sulfur to selenium and tellurium, there are significant increases in rate constant; from sulfur to selenium this increase is often 2 to 3 orders of magnitude, with a similar change observed in progressing from

rad007

Table 1 Representative rate constant data at 80 °C for homolytic ring closures of sulfides, selenides, and tellurides.

Entry	Radical	Solvent	k_c (s^{-1})	Arrhenius[a]	References
1	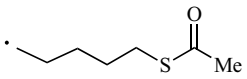	PhH[b]	$\sim 7 \times 10^1$	n.d	14
2	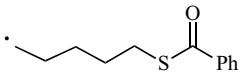	PhH[b]	$\sim 4 \times 10^2$	n.d.	14
3	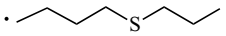	*t*-BuPh[c]	4.4×10^2	$(10.2 \pm 0.6)–(51 \pm 4)/\theta$	15
4	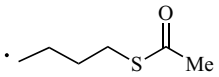	PhH[b]	$\sim 1 \times 10^3$	n.d.	14
5	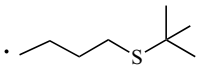	*t*-BuPh[c]	6.9×10^3	$(10.8 \pm 0.2)–(47 \pm 2)/\theta$	15
6	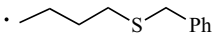	*t*-BuPh[c]	3.7×10^4	$(9.9 \pm 0.2)–(36 \pm 2)/\theta$	15
7	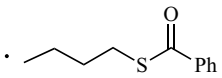	PhH[b]	$\sim 2 \times 10^4$	n.d.	14
8	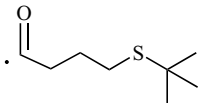	PhH	6.7×10^4	n.d.	16
9	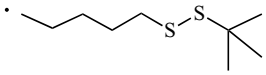	PhH[b]	1.4×10^6	n.d.	14
10	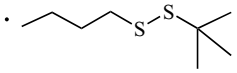	PhH[b]	2.9×10^7	n.d.	14
11	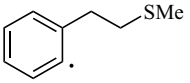	PhH	$\sim 5 \times 10^7$	n.d.	12
12	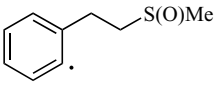	PhH	$>3 \times 10^8$	n.d.	12
13	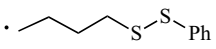	PhH[b]	4.3×10^8	n.d.	14
14	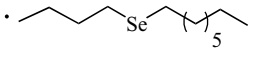	PhH[c]	2.2×10^5	$(9.5 \pm 0.6)–(28 \pm 4)/\theta$	17, 18

(*continued overleaf*)

Table 1 (*continued*)

Entry	Radical	Solvent	k_c (s^{-1})	Arrhenius[a]	References
15	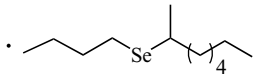	PhH[c]	1.1×10^6	$(9.3 \pm 0.5)–(22 \pm 3)/\theta$	17, 18
16	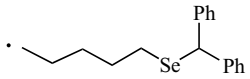	*t*-BuPh[c]	4.3×10^6	$(8.9 \pm 0.1)–(15.3 \pm 0.6)/\theta$	19
17	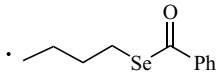	PhH[c]	7.3×10^6	n.d.	17, 18
18	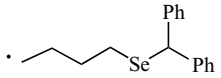	*t*-BuPh[c]	2.1×10^7	$(8.9 \pm 0.2)–(10.6 \pm 0.8)/\theta$	19
19	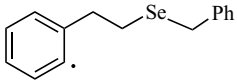	PhH	$\sim 3 \times 10^7$	n.d.	20
20	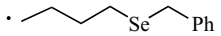	MeCN	6.3×10^7	n.d.	(A. N. Hancock, J. Tanko, and C. H. Schiesser, unpublished)
21	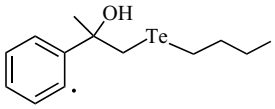	THF	$>10^9$	n.d.	21

THF, tetrahydrofuran; n.d., not determined.
[a] Arrhenius function in kJ mol^{-1}; $\theta = 2.3RT$ kJ mol^{-1}.
[b] Rate constant adjusted from original temperature assuming logA = 10.
[c] Rate constant determined from Arrhenius expression.

selenium to tellurium, although there is only one example of the latter in the list. This trend is attributable to the size of the orbitals involved in the substitution process, with the larger orbitals provided by selenium and tellurium clearly preferred by the attacking radical to those offered by sulfur.

The choice of leaving group is also critical, although this can be somewhat negated by the heteroatom undergoing substitution, as discussed above. The usual reactivity order is observed with $1^\circ < 2^\circ < 3^\circ <$ Bz < Bn < Ph_2C < RS. It is interesting to note that judicious choice of leaving group can turn a poor reaction (e.g., Entry 3) into an excellent reaction (e.g., Entry 10) and this should be kept in mind when designing synthesis based on this chemistry.

In a similar manner to that observed for intramolecular homolytic addition chemistry, and for similar reasons, the size of the ring being formed has an influence on the rate constant because it affects the energy of the transition state involved in ring closure. Five-membered transition states are most favorable because the required collinear arrangement of attacking and leaving radicals is more easily accommodated with four bridging atoms than with the five involved in the formation of the analogous six-membered ring.[8] As can be seen from the data in Table 1, six-membered rings are often formed 1 to 2 orders of magnitude more slowly than their five-membered counterparts.

Despite providing guidance, the data in Table 1 do not provide any information about competing side-reactions. The most common side-reaction is 1,*n*-hydrogen transfer from the "leaving group" to the incoming radical, an example of which is provided in Scheme 6.[15] Benzylic leaving groups

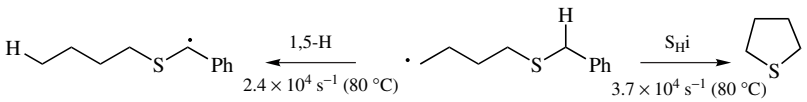

Scheme 6 Hydrogen transfer often competes with homolytic substitution at sulfur.

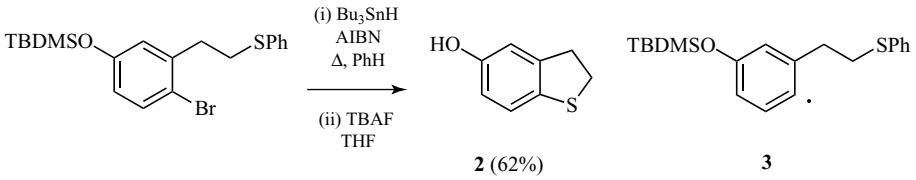

Scheme 7 An example of homolytic ring closure at sulfur with an aryl leaving group.

on sulfur are not suitable for this chemistry; the relatively slow homolytic substitution process at sulfur provides excellent conditions for hydrogen transfer to be competitive. For this reason, *tert*-butyl or thiyl leaving groups are recommended for sulfur. With faster reactions at selenium, benzylselenides are excellent substrates for constructing selenium-containing heterocycles; competing hydrogen transfer in these systems is typically not observed.[20]

Having established some fundamental principles and with an understanding of the kinetics of homolytic substitution processes, examples of synthetically useful chemistry involving sulfur, selenium, and tellurium are now presented.

3.2 Ring Closures at Sulfur

Intramolecular homolytic substitution at sulfur has received considerable attention, and there are several reports in the literature that provide reliable methods for the synthesis of sulfur-containing heterocycles. Examples can be found of alkyl, aryl, and acyl radicals undergoing this chemistry efficiently at the sulfur atom in sulfides,[5] sulfoxides,[12,22,23] sulfinates,[24–26] and sulfonamides,[24–26] but not at sulfones.[22,27]

Scheme 7 illustrates the application of this chemistry to the preparation of the dihydrobenzothiophene-containing tocopherol-like antioxidant (**2**); α-tocopherol is the main component of vitamin E. In the key step, aryl radical (**3**), generated under standard conditions, was able to undergo homolytic substitution at sulfur; subsequent deprotection gave 5-hydroxy-2,3-dihydrobenzo[*b*]thiophene (**2**) in 62% yield over two steps.[28] It is interesting to note that in this example, because the attacking radical is aryl, even the normally unfavorable phenyl radical can be encouraged to act as a leaving group.

Ryu and coworkers reported examples of the preparation of γ-thiolactones (e.g., **4a**) through the application of homolytic substitution by acyl radicals (**5**) at sulfur.[16] The acyl radicals were generated from the corresponding acyl phenylselenide, or through the application of radical carbonylation chemistry developed in their laboratories. In the latter examples, abstraction of the bromine or iodine gives the alkyl radical (**6**) which, under a high-pressure atmosphere of carbon monoxide, forms the corresponding acyl radical (**5**) that then undergoes substitution at sulfur to give the γ-thiolactones (**4**) with expulsion of the *tert*-butyl radical (Scheme 8).

Systems examined include primary and secondary alkyl radicals generated from either bromides or iodides with good leaving groups at sulfur. The best results were obtained for the starting materials shown below. γ-Thiolactones were prepared in 86 and 75% yields from **7** and **8** respectively, while secondary iodides **9** and **10** gave the corresponding γ-thiolactones in moderate yields (Figure 1).[16]

A typical example of the application of this chemistry is in the preparation of **4 d** from 1-(*tert*-butylthio)-2-(iodomethyl)hexane (**7**). In this case, **7** (316 mg, 1.00 mmol), *n*-tributyltin hydride (351 mg, 1.20 mmol), and AIBN (33 mg, 0.2 mmol) were dissolved in benzene (100 ml) in a 200-ml stainless steel autoclave equipped with an inserted glass liner. The vessel was pressurized to 80 atm and heated to 100 °C for 2 h. The autoclave

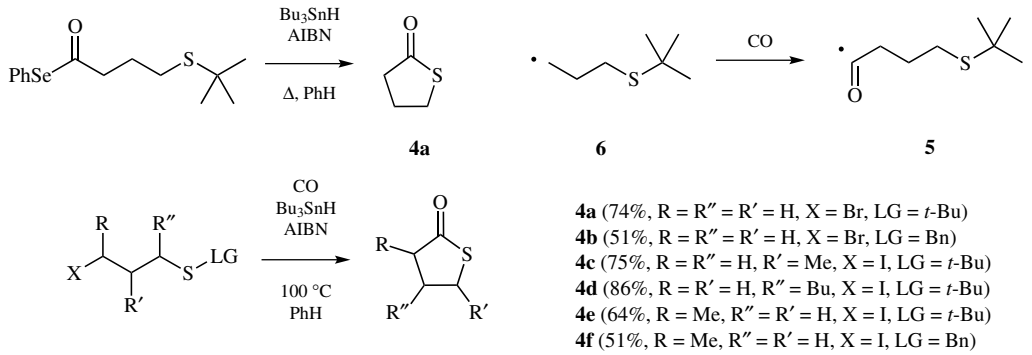

Scheme 8 Examples of ring closures by acyl radicals at sulfur.

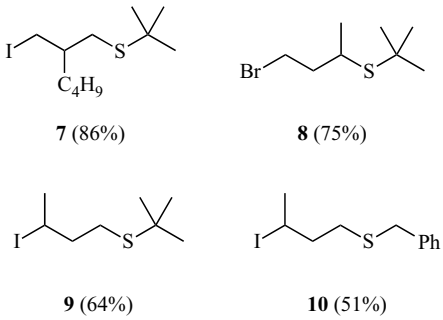

Figure 1 Substrates for the preparation of γ-thiolactones by radical carbonylation/homolytic substitution methodology.

was cooled to room temperature and the pressure released before the solvent was removed *in vacuo*. β-Butyl-γ-thiobutyrolactone (**4 d**) was obtained (135 mg, 86%) after column chromatography.

This methodology was further extended to include α,β-unsaturated acyl radicals, as well as acyl radicals generated from aryl radicals, to yield the corresponding thiolactones (e.g., **11, 12**) in good yields (Scheme 9).[16]

There are few examples of radical substitution reactions involving oxidized sulfur. An early report

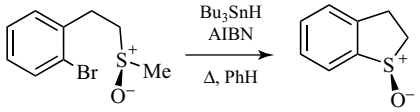

Scheme 10 Chiral sulfoxides undergo homolytic substitution with inversion of configuration.

by Beckwith and Boate showed that these reactions proceed with inversion of configuration, consistent with the backside mechanism discussed above (Scheme 10).[12]

More recently, Malacria and coworkers reported the use of this chemistry at sulfinates and sulfinamides to afford interesting sultines and cyclic sulfinamides (**13**).[24,25] As shown in Scheme 11, a number of variables were explored during their investigation; these included the nature of the (precursor) halide (X), the nature of the aryl ring (Y), the substitution (Z) on the tether, as well as the nature of the leaving radical (LG).

The best results were observed for the starting materials shown below. The nature of the halide did not appear to influence the efficiency of the reaction; however, the leaving radical (LG) proved to be important with *tert*-butyl giving the highest yields

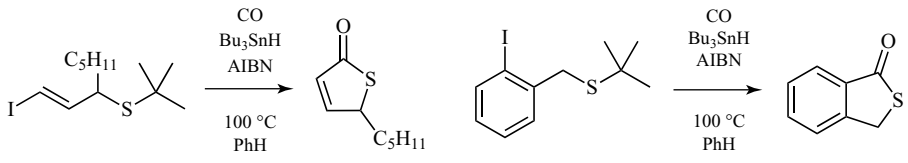

Scheme 9 Vinyl and aryl radicals are efficient in radical carbonylation/homolytic substitution chemistry.

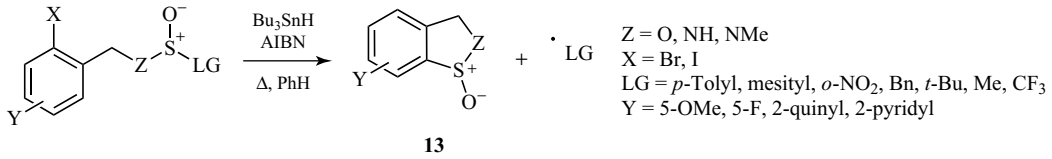

13

Scheme 11 Sulfinates and sulfinamides undergo efficient homolytic substitution by aryl radicals.

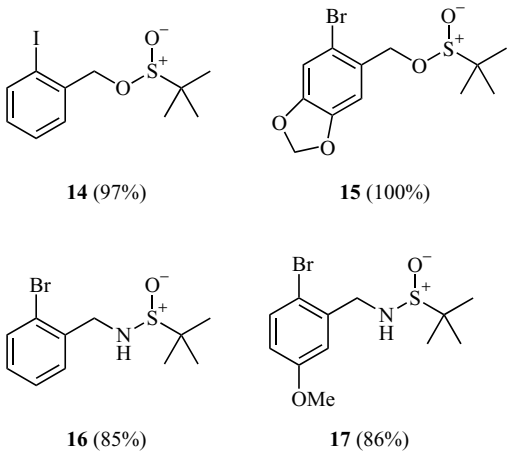

14 (97%) **15** (100%)

16 (85%) **17** (86%)

Figure 2 Key substrates for radical ring closures in sulfinates and sulfinamides.

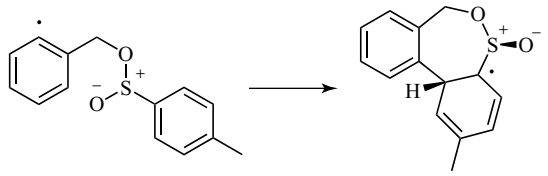

Scheme 12 Homolytic addition often competes with homolytic substitution when aryl leaving groups are used in sulfinates.

of product. Primary, benzyl, and trifluoromethyl leaving radicals proved to be less efficient. The nature of the aryl group was also investigated and this study concluded that electron-donating groups (Y) on the aryl ring were beneficial; however, electron-withdrawing groups were also tolerated, as were thiophenes. For example, sulfinates **14** and **15** led to the synthesis of the corresponding sultines (**13**, $Z = O$) in 97% and quantitative yields respectively, while cyclic sulfinamides (**13**, $Z = NH$) were prepared in 85 and 86% yields from **16** and **17**, respectively (Figure 2).

It should be noted that with aryl leaving groups (LG), intermolecular addition to LG is reported as being a competitive process, an example of which is depicted in Scheme 12.[24,25]

Malacria also reported the use of alkyl radicals in substitution chemistry at sulfinates.[24,25] Primary, secondary, and tertiary radicals, generated from the corresponding bromide, were all successfully employed. It should be noted that when a secondary alkyl radical is used, a new stereogenic center is created, with the size of the new substituent influencing selectivity; the trans diasteroisomer is favored in all such examples. These alkyl sultine scaffolds are small molecule natural products that exhibit interesting olfactory and flavor properties. For example, sultine (**18**) is found in passion fruit extracts and was prepared in a 9 : 1 trans : cis mixture of diastereomers by reaction of the secondary bromide (**19**) with tris (trimethylsilyl)silane (Scheme 13),[25] while sultine (**20**) was formed from a tertiary radical under standard radical conditions; this compound is a component of cat's urine.[29]

3.3 Ring Closures at Selenium and Tellurium

Radical cyclization chemistry involving selenium is generally easier to conduct than its sulfur counterpart because of the more-favorable rate constants for homolytic attack at selenium over sulfur (Table 1); consequently, since its "discovery" in the early 1990s,[20,30,31] there have been numerous examples of this chemistry, mainly from our laboratories.[3,17,32–35] In the case of selenium, the benzyl radical has generally been the leaving group of choice, and its use in selenium chemistry is not complicated by competing 1,*n*-hydrogen transfer chemistry because the substitution process is some 2 to 3 orders of magnitude faster than that for the similar reaction involving sulfur.[20] However, because of the increased reactivity of the selenium atom toward radicals, that include chain-carrying radicals such as *n*-tributylstannyl,[2] most of the

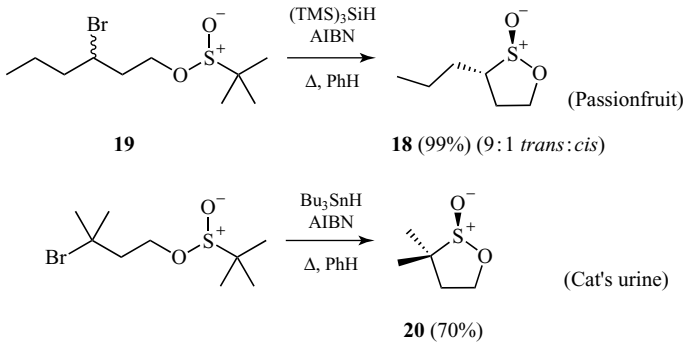

Scheme 13 Alkyl radicals give rise to interesting sultines, sometimes with excellent stereocontrol.

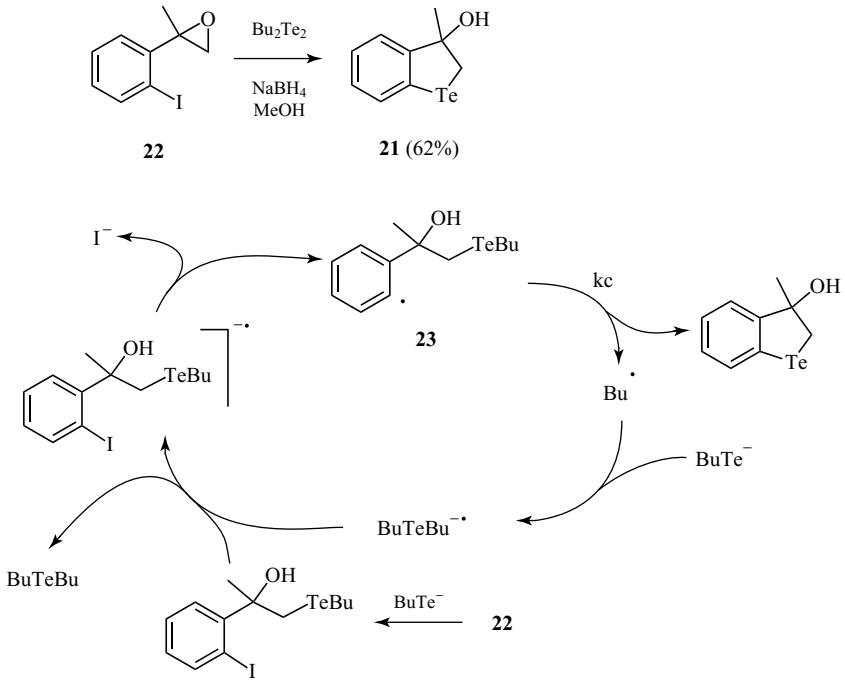

Scheme 14 Formation of dihydrobenzo[*b*]tellurophenes by intramolecular homolytic substitution chemistry.

synthetically useful homolytic chemistry carried out at selenium has utilized the (more reactive) iodide (over the bromide) as radical precursor, or has made use of precursors that do not require chain-carriers.[30,31,33–39]

In contrast, there are relatively few examples of intramolecular homolytic substitution reactions at tellurium, and this can be attributed to a number of factors that include (i) the intrinsic photolability of organic tellurides, (ii) the propensity for organic tellurides to react with oxygen, and (iii) their intrinsic reactivity toward chain-carrying radicals; indeed organic tellurides are often more reactive toward radicals such as *n*-tributylstannyl, than are the corresponding iodides.[2,21] Nevertheless, there are some examples of this chemistry (see below), and success required the invention of new ways of generating radicals in the presence of tellurium, in particular, the use of aryl iodides together with sodium *n*-butyltellurolate.[21,40]

In the example provided in Scheme 14, 2, 3-dihydro-3-hydroxy-3-methylbenzo[*b*]tellurophene

21 was isolated in 62% yield upon treatment of the aryl iodide (**22**) with sodium *n*-butyltellurolate generated *in situ*.[21,40] Under these reaction conditions (in the dark) **22** undergoes single-electron transfer to generate the aryl radical **23**, which undergoes homolytic substitution at tellurium to give the required product.[40] It should be noted from the data in Table 1 that the nature of the leaving group at tellurium is essentially irrelevant in this chemistry because even the *n*-butyltelluride (last entry) ring closes with a rate constant in excess of 10^9 s^{-1} at 80 °C.[21]

The experimental procedure for the preparation of **21** is as follows: sodium borohydride (47 mg, 1.24 mmol) was added to a solution of di-*n*-butyl ditelluride (216 mg, 0.59 mmol) in tetrahydrofuran (2 ml). The reaction vessel was purged with nitrogen, and methanol (circa 1 ml) was added dropwise, with caution, until a persistent pale yellow solution was obtained. 1-(2-iodophenyl)-1-methyloxirane (**22**) (118 mg, 0.45 mmol) in tetrahydrofuran (1 ml) was added rapidly and the resultant mixture was stirred overnight, shielded from background light. Following aqueous work up, the residue was purified by column chromatography to give 2,3-dihydro-3-hydroxy-3-methyl-benzo[*b*]tellurophene(**21**) as a yellow solid (74 mg, 62%) with a melting point of 71–73 °C.

This methodology was also successfully applied to the preparation of tocopherol-like antioxidants containing selenium (**24**) and tellurium (**25**) in yields of 65 and 47%, respectively (Scheme 15).[40]

Intramolecular homolytic substitution at selenium was the key step in the synthesis of selenotocopherol reported by Engman *et al*.[41] As shown in Scheme 16, the alcohol (**26**) was reacted with oxalyl chloride followed by 2-mercaptopyridine N-oxide. The pyridine-2-thioneoxycarbonyl (PTOC) imidate ester precursor (**27**) was formed *in situ* and upon heating gave the selenochroman (**28**) presumably by through a process involving the tertiary radical **29**. Subsequent deprotection of **28** with borontrifluoride gave the racemic selenotocopherol.

The use of thiohydroximidate esters (PTOC, Barton, Kim esters) as carbon-centered radical precursors has the advantage that chain-carrying radicals such as *n*-tributylstannyl ("standard radical conditions", **Basic Concepts on Radical Chain Reactions**, Volume 1) can be avoided.[31,38,39] In a rad017

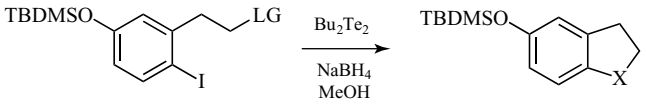

24 (65%, LG = SeBn, X = Se)
25 (47%, LG = I, X = Te)

Scheme 15 Formation of selenium and tellurium heterocycles mediated by sodium *n*-butyltellurolate.

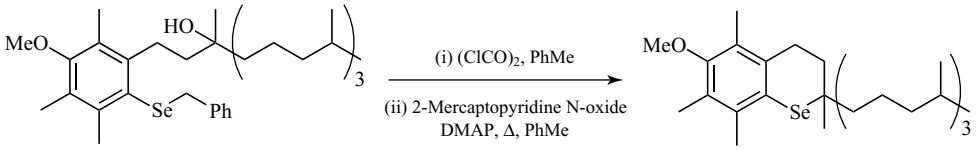

26 **28** (49%)

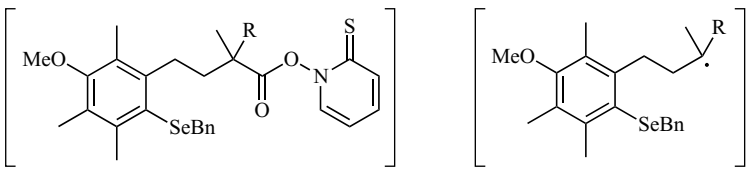

27 **29**

Scheme 16 Formation of selenotocopherol through the use of intramolecular homolytic substitution chemistry involving selenium.

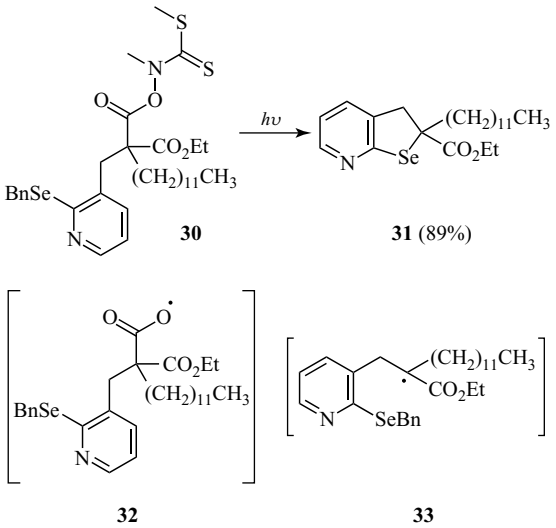

30 **31** (89%)

32 **33**

Scheme 17 Formation of 2,3-dihydroselenolo[2,3-b]pyridines by intramolecular homolytic substitution chemistry.

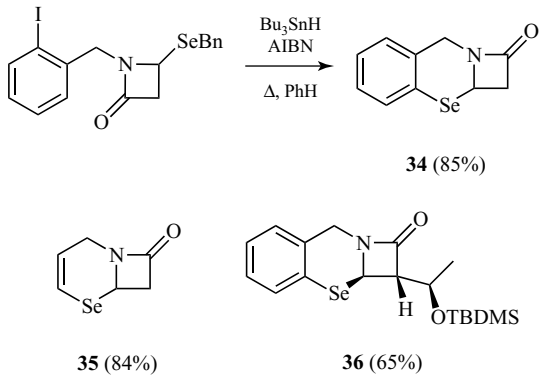

34 (85%)

35 (84%) **36** (65%)

Scheme 18 Selenacephems can be prepared by radical ring-closure chemistry involving selenium.

further example, Fenner demonstrated that photolysis of the thiohydroximate (Kim) ester (**30**) afforded the pyridine-fused selenophene (**31**) in 89% yield.[39,42] Presumably, this transformation involves cleavage of the nitrogen–oxygen bond to give the acyloxyl radical **32**; rapid decarboxylation generates the tertiary radical **33**, which undergoes further homolytic substitution at selenium (Scheme 17).

The synthesis of selenapenam and selenacephalosporin "core" structures as compounds of biological interest was achieved by Carland and Martin through the use of intramolecular homolytic substitution of aryl, vinyl, and alkyl radicals at selenium in suitably substituted 4-benzylseleno-β-lactams.[38,43] For example, under standard radical conditions, the benzo-fused selenium-containing heterocycle **34** was prepared in 85% yield (Scheme 18). Under similar conditions both selenium-containing heterocycle **35** and selenapenam **36** were synthesized in 84 and 65% yields, respectively.

Thiohydroximate esters were also successfully employed as precursors in the synthesis of optically active selenium analogs of β-lactam antibiotics. As shown in Scheme 19, the selenapenam **37** was formed in 51% yield upon irradiation. The selenium-containing heterocyclic core (**38**) of the β-lactamase inhibitor, sulbactam (**39**) was prepared under similar conditions as a mixture of diasteroisomers which epimerized to a single compound upon standing.[38]

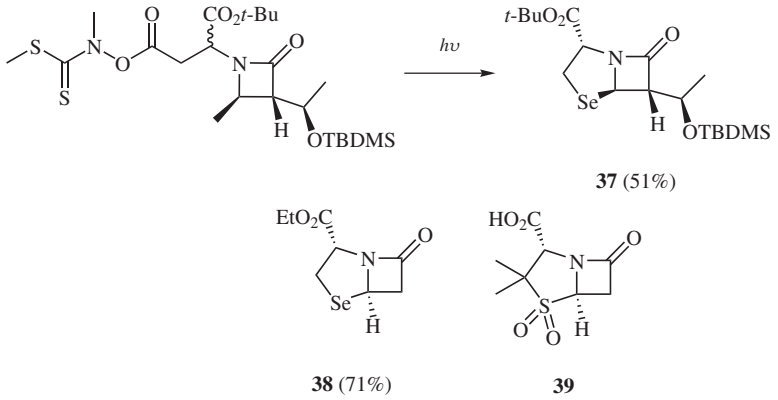

37 (51%)

38 (71%) **39**

Scheme 19 Selenium analogs of the β-lactamase inhibitor, sulbactam, can be prepared by homolytic substitution chemistry.

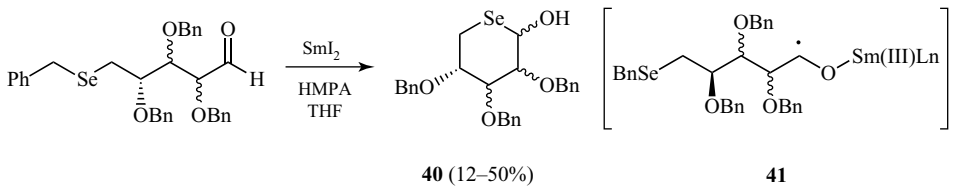

40 (12–50%) **41**

Scheme 20 Samarium iodide-mediated homolytic substitution chemistry can lead to selenium analogs of pyranose carbohydrates.

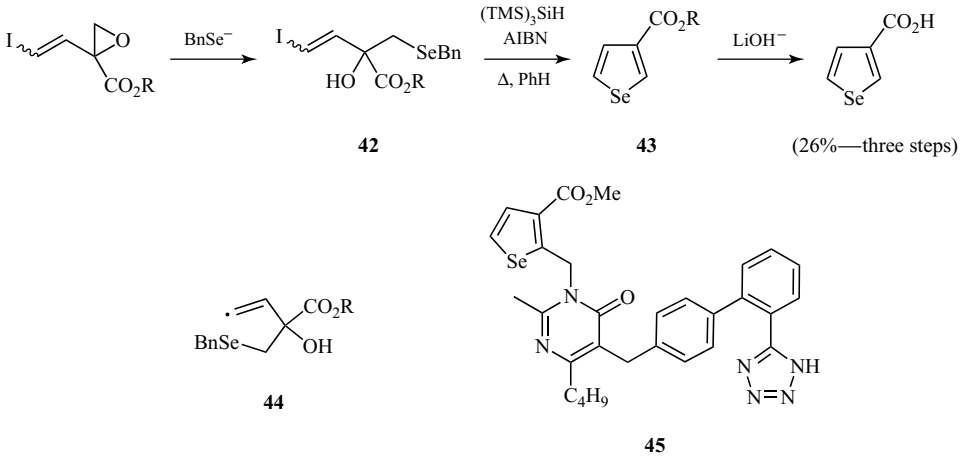

42 **43** (26%—three steps)

44 **45**

Scheme 21 Intramolecular homolytic substitution chemistry is the key step in the synthesis of *selenomilfasartan*, a potent angiotensin AT_1 receptor antagonist.

In an attempt to make water-soluble antioxidants, Zheng showed that a series 5-selenapentopyranose derivatives (**40**) could be prepared in low to moderate yields by samarium(II) iodide-mediated radical chemistry as depicted in Scheme 20.[44,45] The key step in this chemistry involves cyclization at selenium of the samarium-containing radical (**41**).

More recently, radical cyclization reactions involving selenium have been employed in the synthesis of analogs of selective AT_1 receptor antagonists (*sartans*). In particular, Grange showed that treatment of iodide (**42**) with tris(trimethylsilyl)silane gave the selenophene-3-carboxylate (**43**) (Scheme 21),[32] presumably through the action of the vinyl radical (**44**). Subsequent chemistry led to the synthesis of *selenomilfasartan* (**45**) which proved to be a more potent antagonist than the parent thiophene analog, *milfasartan*.[32]

To the best of our knowledge, there is only one reported example of an oxyacyl radical involved in substitution chemistry at selenium. Lucas reported that, upon irradiation, telluroformate (**46**) affords the cyclic selenocarbonate (**47**) in 73% yield, presumably through the involvement of radical **48** (Scheme 22).[36]

3.4 Tandem Radical Sequences Involving Homolytic Substitution at Selenium

The application of tandem (cascade) radical chemistry to the preparation of interesting molecules is now accepted as a common place by the synthetic practitioner because it allows for the rapid one-pot construction of multiple bonds; other articles of this work are devoted to this chemistry (**Radical Cascade Reactions**, Volume 2). Until recently, however, there were no reported examples of tandem radical chemistry that included intramolecular homolytic substitution of a selenium atom as a key component of the overall sequence. rad022

As shown in Scheme 23, it is possible to construct tandem sequences involving intermolecular homolytic addition followed by substitution. The chemistry depicted in Scheme 23 makes

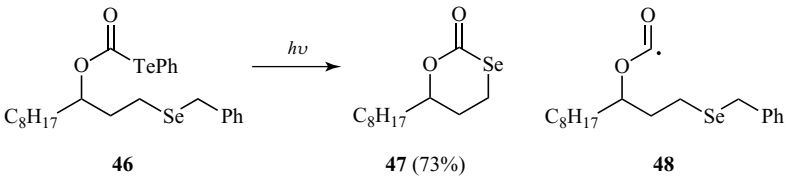

46 **47** (73%) **48**

Scheme 22 Ring closure by oxyacyl radicals at selenium can lead to interesting cyclic selenocarbonates.

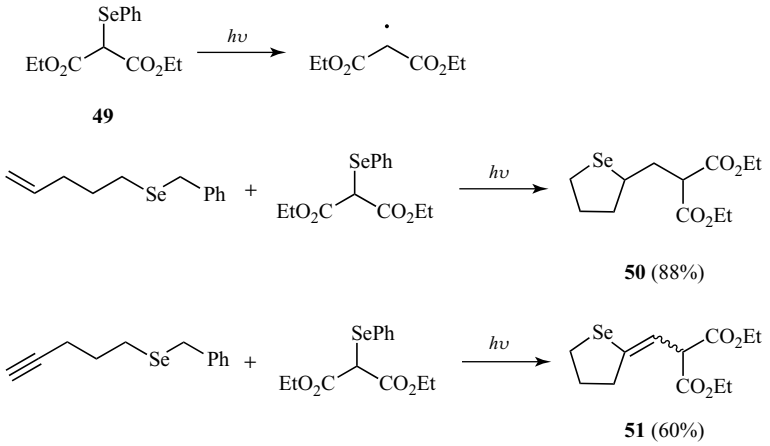

49

50 (88%)

51 (60%)

Scheme 23 Examples of tandem homolytic addition/substitution sequences involving selenium.

use of the photochemical lability of diethyl 2-(phenylseleno)malonate (**49**),[46] which, upon irradiation, affords the diethyl malonyl radical. Subsequent addition at terminal alkenes or alkynes, followed by substitution at selenium gave the tetrahydroselenophenes (**50, 51**) in 88 and 60% yields, respectively.[47] Other leaving groups were examined, with substrates **52**–**54** providing **50** in good to moderate yields, as depicted in Figure 3.

In a further recent example of this chemistry, Staples showed that selenochromanes can be

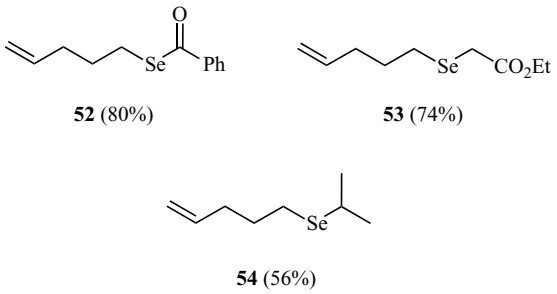

52 (80%) **53** (74%)

54 (56%)

Figure 3 Some substrates for tandem homolytic addition/substitution chemistry.

conveniently prepared through a tandem radical sequence involving intermolecular addition by benzylic radicals to suitably substituted alkenes, followed by intramolecular homolytic substitution at selenium. For example, irradiation of the dithiocarbonate (**55**) in the presence of methyl acrylate afforded **56** in 40% yield (Scheme 24).[33] This reaction presumably proceeds through the involvement of the radical (**57**) which adds to methyl acrylate; the adduct radical then undergoes homolytic substitution at selenium to give the observed product.

As shown in Scheme 25, this chemistry can be initiated using triethylborane/oxygen at lower temperatures; however, these reactions now require significantly electron-withdrawn alkenes to be effective; for example, *N*-benzyl maleimide gave selenochromane **58** in 71% yield. This methodology was also employed in the synthesis of the nitro-substituted and pyridyl selenochromanes **59** and **60** in good to moderate yields.

A typical protocol for one of these tandem reactions is illustrated in the synthesis of selenochromane **56**. In this case, *O*-ethyl-*S*-(2-(benzylseleno)benzyl) dithiocarbonate (**55**) (209 mg, 0.55 mmol) and methyl acrylate

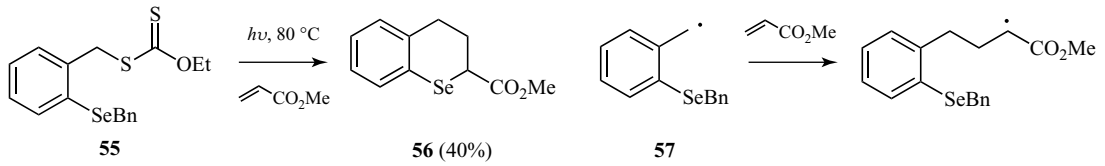

Scheme 24 Preparation of the selenochromane ring system using tandem radical chemistry.

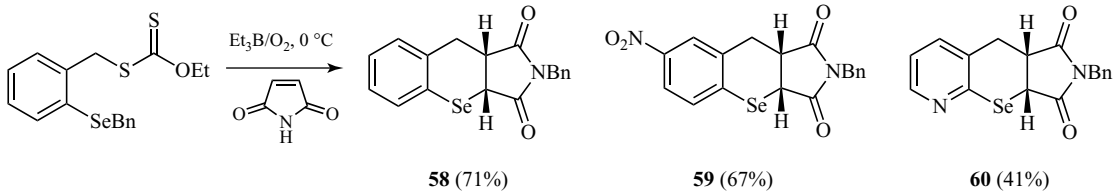

Scheme 25 Examples of selenochromanes prepared by radical cyclization chemistry.

(76 ml, 0.82 mmol) were dissolved in toluene (1.5 ml) in a Pyrex tube after "degassing" by bubbling a steady stream of nitrogen through the solvent. The reaction vessel was sealed and irradiated for 12 h with a 125-W medium pressure mercury lamp at a distance of 15 cm while maintaining the temperature at 80 °C. Methyl 3,4-dihydro-2*H*-1-benzoselenin-2-carboxylate (**56**) was purified by column chromatography (5% ethyl acetate/petroleum spirits) to afford a colorless oil (0.22 mmol, 40%).[33]

Staples was able to extend this novel tandem addition/substitution methodology to the preparation of benzo[*b*]selenophenes, an example of which is depicted in Scheme 26.[34] It should be noted that this chemistry requires the involvement of an alkane bearing an electron-withdrawing group and was inspired by the contributions of Zanardi and coworkers toward the construction of benzo[*b*]thiophenes.[48] Presumably, the diazonium salt (**61**) reacts in the presence of iron to generate the aryl radical (**62**), which then

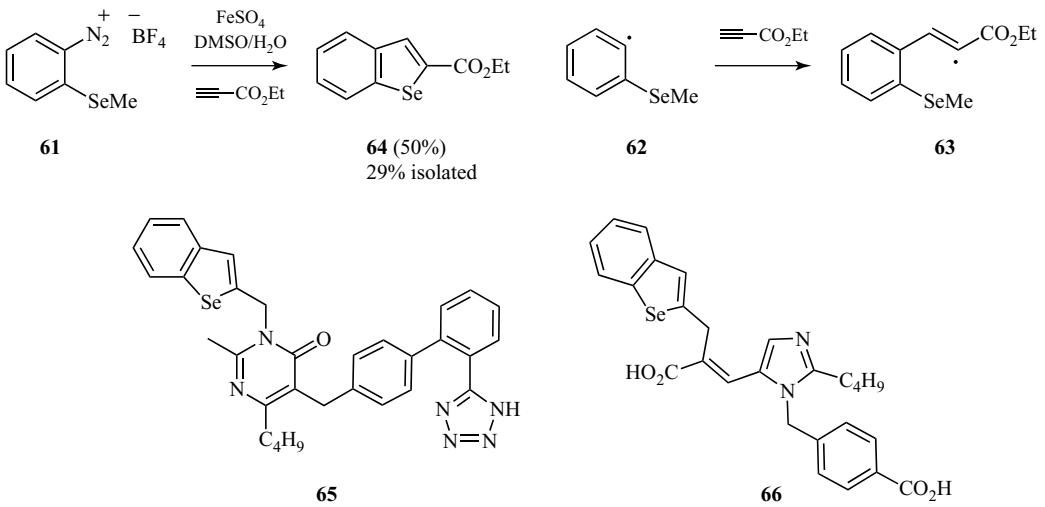

Scheme 26 Selenium-containing angiotensin AT_1 receptor antagonists can be prepared by tandem homolytic addition/substitution chemistry.

undergoes intermolecular addition onto the alkyne. The adduct(vinyl) radical (**63**) reacts at selenium to give ethyl benzo[*b*]selenophene-2-carboxylate (**64**) in 50% yield (29% isolated yield). Despite the moderate yield, this one-pot procedure represents a significant improvement over traditional multi-step methods for the preparation of benzoselenophenes.[49,50] Key intermediate **64** was incorporated into benzo[*b*]selenophene analogs (**65**, **66**) of the antihypertensive drugs, *milfasartan* and *eprosartan*.[34]

4 INTRAMOLECULAR HOMOLYTIC SUBSTITUTION AT OXYGEN

Homolytic substitution at unactivated oxygen is relatively rare because of a mismatch of orbital overlap between the attacking radical and the oxygen atom. However, several examples exist of this chemistry taking place at oxygen atoms that are activated by strain or by a metal, or in peroxides that contain intrinsically weak oxygen–oxygen bonds.[2,51,52]

Nugent and RajanBabu showed that epoxides can be used as radical precursors that can undergo electron transfer when treated with stoichiometric titanocene dichloride (see **Epoxides in Titanocene-Mediated and -Catalyzed Radical Reactions**, Volume 2). Ring opening of the epoxide results in the formation of an oxygen–metal bond.[53–56]

rad029

Gansäuer and Grimme *et al*. were able to further develop this methodology to tandem radical chemistry that included a step in which the radical underwent homolytic substitution at oxygen, as depicted in Scheme 27.[57,58] In this example, half an equivalent of 2,4,6-trimethylpyridine hydrochloride is required to liberate Cp_2TiCl_2 which is then reduced by manganese dust (0.2 equiv) to give the reactive species, Cp_2TiCl. Ultimately, the tetrahydrofuran (**67**) was isolated in 67% yield as a single diastereomer through a process presumably involving reductive epoxide ring opening (mediated by the titanocene(III) complex), 5-exo cyclization and homolytic substitution at oxygen.

The effect of substitution of the alkene was investigated and a variety of different products were successfully synthesized under conditions similar to those in Scheme 27. The tricyclic compound (**68**) was obtained as a single isomer in 73% yield. Both the 1,3-dithiane (**69**) and diethyl malonate (**70**) systems gave similar results with the products isolated in 65 and 62% yields, respectively. Styrene substrates were also explored as radical acceptors

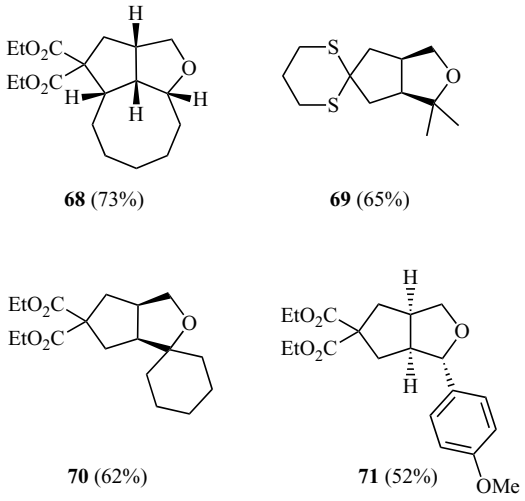

68 (73%) **69** (65%)

70 (62%) **71** (52%)

Figure 4 Examples of tetrahydrofurans prepared by titanium-mediated radical chemistry.

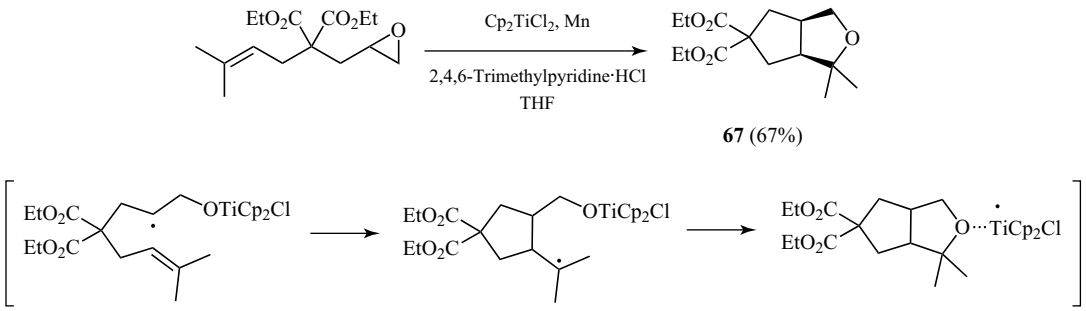

67 (67%)

Scheme 27 Titanium-mediated homolytic substitution chemistry involving oxygen can lead to the formation of tetrahydrofurans.

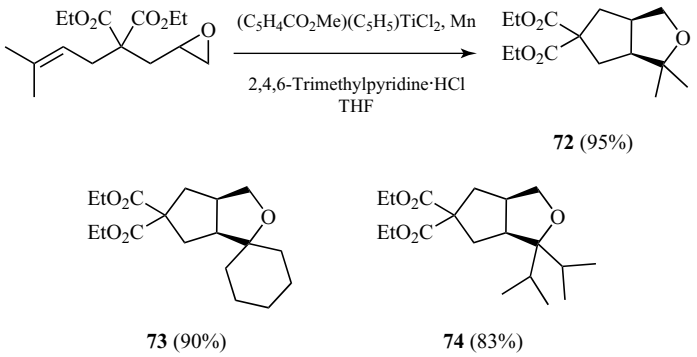

Scheme 28 Improved procedure for the preparation of tetrahydrofurans by radical cyclization at oxygen.

leading to the synthesis of **71** in 52% yield (Figure 4).

Further improvements to the reaction's synthetic utility were made in a more recent study (Scheme 28).[59] Increasing reaction temperature was found to be beneficial, while a computational investigation resulted in an improvement to the catalyst being made; indeed a catalyst with increased Lewis acidity was identified to favor epoxide binding and resulted in an improvement in the product yield. Using this new procedure, tetrahydrofuran **72** was isolated in 95% yield, while key compounds **73** and **74** were isolated in 90 and 83% yields, respectively. The yield of **74** is particularly noteworthy because it is sterically hindered; indeed **74** was not formed when the original conditions were employed.

The protocol for this chemistry is illustrated by the synthesis of **72** as follows: the titanocene catalyst (61.2 mg, 0.200 mmol), collidine hydrochloride (158 mg, 1.00 mmol), and manganese dust (22 mg, 0.400 mmol) were heated under vacuum until the collidine hydrochloride began to sublime slightly before use. Then dry tetrahydrofuran (20 ml) and the epoxide (568 mg, 2.00 mmol) were added and the mixture stirred at 95 °C for 4 h. After addition of *tert*-butyl methyl ether (10 ml), the mixture was washed with 2 M hydrochloric acid (10 ml), the aqueous layer was extracted with CH_2Cl_2 (2×10 ml) and *tert*-butyl methyl ether (10 ml). The combined organic layers were washed with brine (10 ml) and dried ($MgSO_4$). The solvents were removed under reduced pressure and the crude product was purified by column chromatography to afford **72** (597 mg, 95%) as a 5 : 1 mixture of diastereoisomers.

5 INTRAMOLECULAR HOMOLYTIC SUBSTITUTION AT SILICON, GERMANIUM, AND TIN

5.1 Homolytic Substitution at Silicon

The first examples of cyclization reactions involving substitution at silicon were reported by Giese and coworkers[60] and Utimoto *et al*.[61] almost 20 years ago; these were included in the 1996 review.[2] Since then, Studer *et al*. studied the effect of aryl radicals at a variety of substituted alkoxysilanes (**75**) as shown in Scheme 29.[62] When

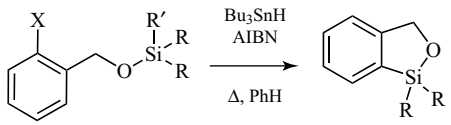

75

76a (5%, X = Br, R = Ph, R′ = $SiPhMe_2$)
76b (91%, X = Br, R = R′ = $SiMe_3$)
76c (80%, X = I, R = Ph, R′ = $SnMe_3$)

Scheme 29 Intramolecular homolytic substitution at silicon can lead to cyclic alkoxysilanes.

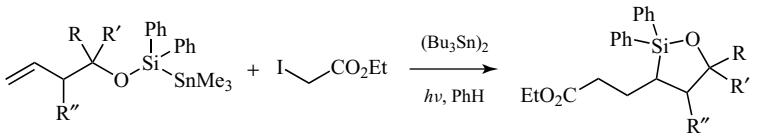

77

78a (19%, R = Ph, R′ = R″ = H)
78b (67%, R = Ph, R′ = Me, R″ = H)
78c (76%, R = R′ = R″ = Me)

Scheme 30 Tandem homolytic addition/substitution for the formation of cyclic alkoxysilanes.

R′ = dimethylphenylsilane the substitution reaction proved difficult. Only 5% of the desired alkoxysilane (**76a**) was isolated, along with 43% of unidentified material. The authors attributed this to the strong Si–Si bond in the starting material. Better results were obtained for the tris(trimethylsilyl)silane (**75b**), leading to **76b**. Addition of sub-stoichiometric *n*-tributyltin hydride (0.5 equiv) through a syringe pump gave 91% of **76b**. The trimethylstannyl-substituted silane could be reacted with 0.2 equiv of *n*-tributyltin hydride (added in two portions) to give alkoxysilane **76c** in 80% yield. Owing to the ease with which the Si–Sn bond could be cleaved it was concluded that stannyl-substituted silanes were most suitable for radical ring-closure chemistry at silicon.[62]

Alkyl radicals have also been cyclized at silicon using similar methods, and tandem radical addition/substitution reactions proved to be particularly effective, enabling the efficient synthesis of alkoxysilanes (**78**) from trimethylstannyl-substituted silanes (**77**) (Scheme 30).[63] These reactions could be conducted in the absence of a hydride source, and this observation led to a photochemical protocol involving sub-stoichiometric hexabutylditin (0.1 equiv). This proved to be a necessary improvement, as alkyl radicals seem to react relatively slowly in their cyclization chemistry at silicon. Stereoselectivity was also investigated and good diastereoselectivity was reported. For example, reaction of ethyl iodoacetate with a racemic silyl ether resulted in the isolation of the *trans*-alkoxysilane (**79**) in 87% yield; **80** and **81** were also isolated in good to moderate yields (Figure 5).[63]

Studer and coworkers also conducted important kinetic experiments and these studies provided the approximate rate constants for radical ring closure at silicon that are listed in Table 2.[63] It should be noted that the data for the slower systems contain substantial errors attributed to low amounts

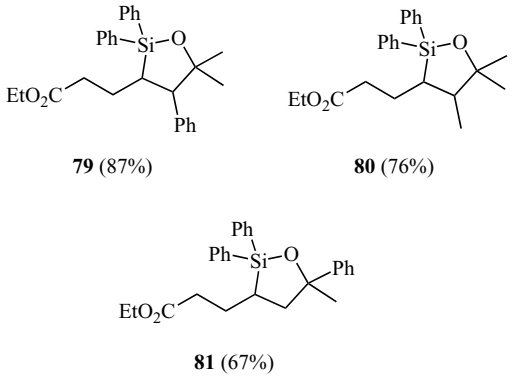

79 (87%) **80** (76%)

81 (67%)

Figure 5 Key silacycles prepared by tandem homolytic addition/substitution.

of cyclized product detected under the reaction conditions; these numbers should be treated with caution, but are nevertheless helpful to practitioners wishing to design syntheses based on this chemistry.

As was observed for the chalcogens, rate constants for cyclization at silicon are strongly dependent on the leaving group. Not unexpectedly, increases in rate constant are observed as the leaving radical stability improves: $SnMe_3 > GeMe_3 > SiMe_3$. With values of k_c in excess of 10^5 s^{-1} at 80 °C, it is not surprising that stannyl-substituted silanes are the best substrates for this chemistry. The other important variable available to silicon that is not available to the chalcogens, is substitution on the heteroatom itself. The data in Table 2 suggest that phenyl and trimethylsilyl substituents are preferred over methyl, presumably because of their stabilizing influence on the transition state during cyclization.

The knowledge gained during these earlier investigations were later exploited by Studer where they successfully coupled intramolecular addition together with homolytic substitution at silicon to achieve a stereocontrolled synthesis of cyclic vinyl

Table 2 Representative rate constant data at 80 °C for homolytic ring closures at silicon (in benzene).[63]

Radical	Leaving group	Product	k_c (s^{-1})
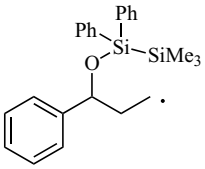	$^{\bullet}SiMe_3$	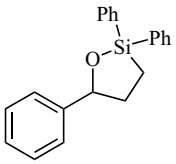	$\sim 10^3$–10^4
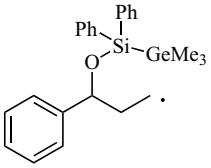	$^{\bullet}GeMe_3$	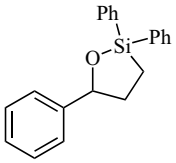	$\sim 1.5 \times 10^4$
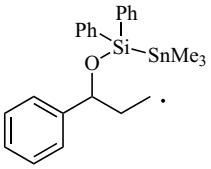	$^{\bullet}SnMe_3$	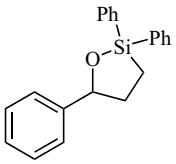	1.2×10^6
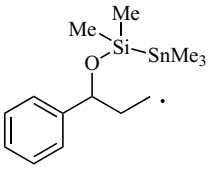	$^{\bullet}SnMe_3$	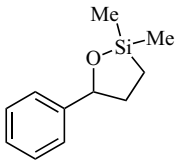	1×10^5
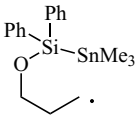	$^{\bullet}SnMe_3$		1.5×10^5
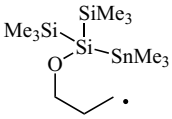	$^{\bullet}SnMe_3$	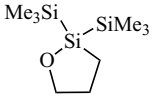	2×10^6

silanes (**82**) (Scheme 31).[64] In this chemistry, abstraction of bromine provides alkyl radicals **83** which undergo 5-exo-dig cyclizations onto the alkyne to give the vinyl radical **84**. These reactive radicals are then able to undergo intramolecular substitution at silicon to afford a variety of bicyclic alkoxysilanes (**82**). The trimethylstannyl radical (leaving group) can be exploited as a radical chain carrier, meaning that these reactions can be conducted with sub-stoichiometric amounts of *n*-tributyltin hydride, often added via syringe pump.

The best results were obtained with phenyl and trimethylsilyl substitution on the vinyl radical providing the corresponding alkoxysilanes (**85** and **86**) in 86 and 84% yields, respectively. In contrast to this, only moderate yields were obtained for the alcohol **87** and the trimethylsilylmethyl-substituted product **88** (Figure 6).

Analogous methodology was applied to vinyl iodides (Scheme 32). The vinyl radicals that are generated following abstraction of the iodine atom in **89** were able to undergo homolytic substitution

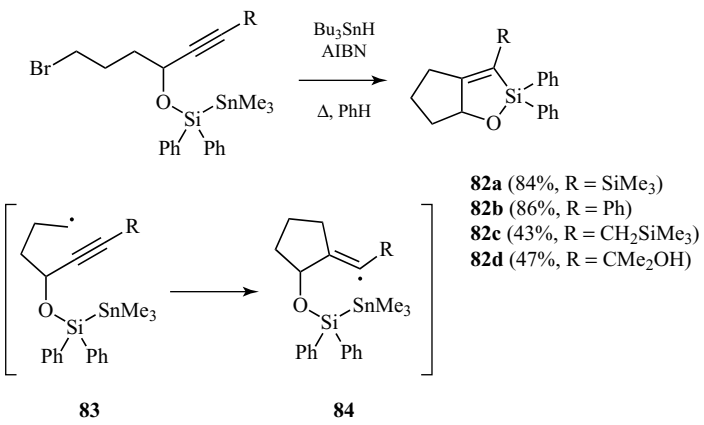

Scheme 31 Vinyl radicals in intramolecular homolytic ring closures at silicon.

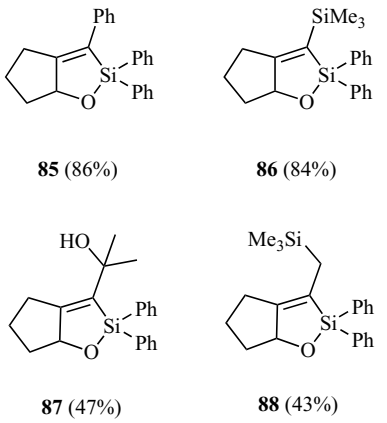

Figure 6 Some key cyclic alkoxysilanes produced through vinyl radical cyclizations at silicon.

at silicon to give the cyclized products which proved too difficult to isolate directly; subsequent treatment of the crude reaction mixtures with excess methyllithium gave the corresponding ring opened vinylsilanes (**90**) in good to moderate yields.

Good stereoselectivity could be obtained when a secondary (**91**, trans : cis 93 : 7) or tertiary (**92**, trans : cis > 98 : 2) group was bound directly to the alkene, these substrates also gave the best yields. In contrast to this, the primary substituent afforded quite poor selectivity with a trans : cis ratio of only 2 : 1 in **93** (Figure 7). It was concluded that trans cyclization was favored as this enabled the R group and trimethylstannyl substituent to avoid coming into close proximity with one another.

Together with Studer, Ryu and coworkers were able to demonstrate the first example of an acyl radical undergoing homolytic substitution at silicon to form a silicon-containing ring (Scheme 33).[65] Abstraction of the bromine atom in **94** gives rise to the alkyl radical (**95**), which under Ryu's carbonylation conditions formed the acyl radical (**96**) which is subsequently able to undergo homolytic substitution at silicon to give diphenylsilacyclopentanone (**97**) and the trimethylstannyl radical. Using *n*-tributyltin

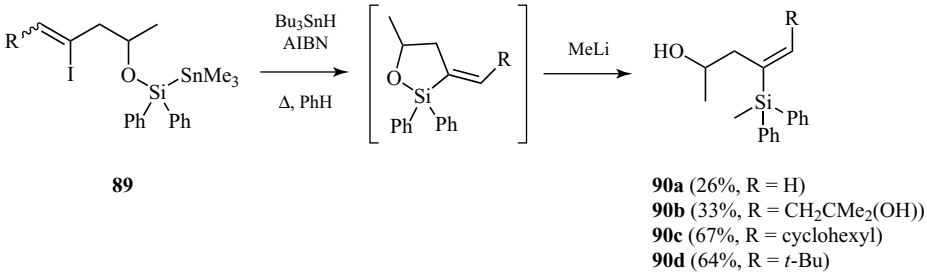

Scheme 32 Some ring closures at silicon from vinyl iodide substrates.

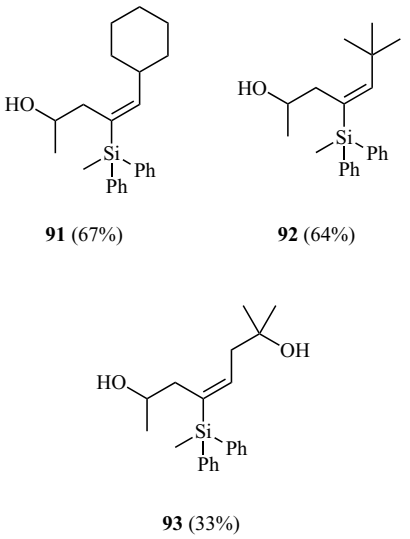

Figure 7 Key products formed from radical precursors **89**.

hydride as the chain carrier, the product (**97**) was isolated in 20% yield; however, these reactions were associated with a variety of side-products. Competition between cyclization at silicon and reduction of the acyl radical was observed. Use of tris(trimethylsilyl)silane (see **Silanes as Reducing Reagents in Radical Chemistry**, Volume 2) suppressed the competitive formation of aldehyde (**98**) and also reduced product (**99**) while increasing the yield of silacyclopentanone to 35%.

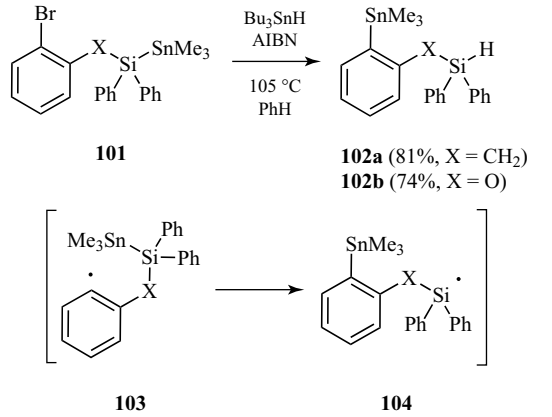

Scheme 34 Examples of 1,4-stannyl migration from silicon to carbon.

Surprisingly, the 1-silyl-3-stannylpropane (**100**) was also isolated from these reaction mixtures in yields of 16–17%. This product can be attributed to the alkyl radical **95** undergoing the alternate frontside homolytic substitution process, resulting in 1,4-stannyl migration; competitive kinetic experiments provided a rate constant ($k_{1,4}$) of $9.3 \times 10^4\ s^{-1}$ (80 °C) for the 1,4-migration of the trimethyltin group from the silicon atom to the carbon in **95**[65]; $k_{1,4}$ is similar to the values of k_c provided in Table 2. Under carbonylation conditions the yields of the 1,4-stannane migration product were only moderate, while in the absence of carbon

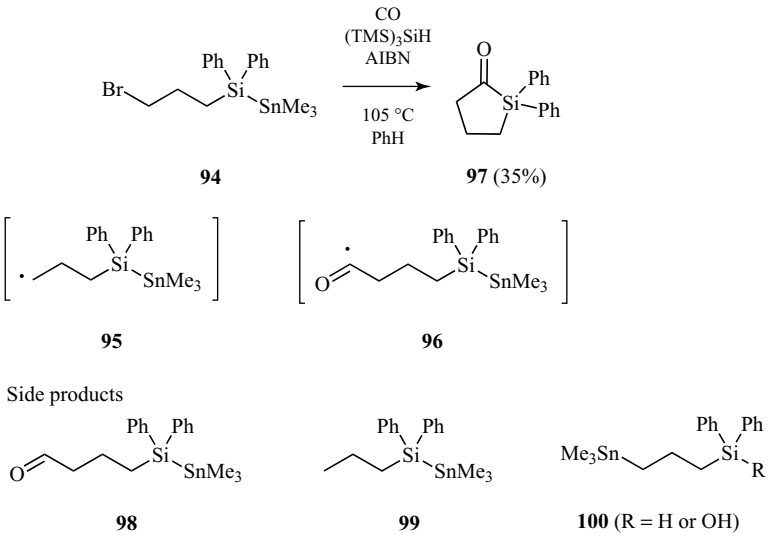

Scheme 33 Radical carbonylation followed by ring closure at silicon is accompanied by several side-products.

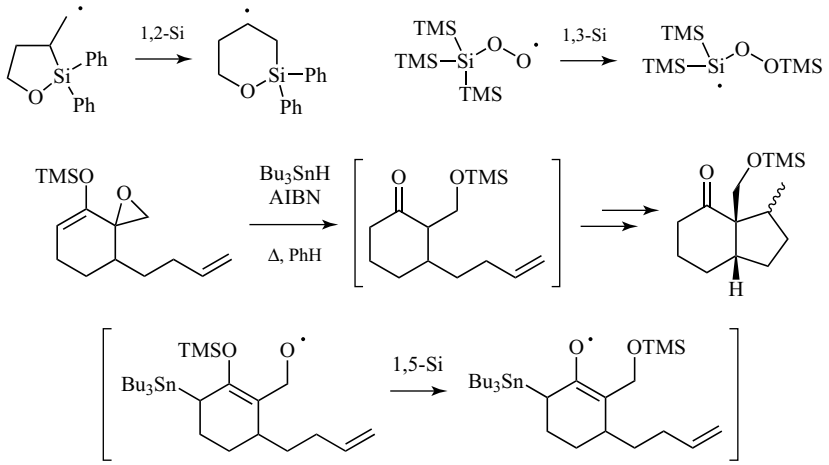

Scheme 35 Some examples of 1,*n*-silyl translocations.

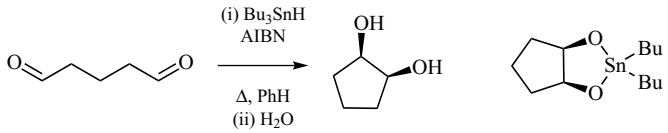

104 **105** (46%) **106**

(98 : 1 *cis* : *trans*)

Scheme 36 Example of a stannane-mediated pinacol-coupling reaction.

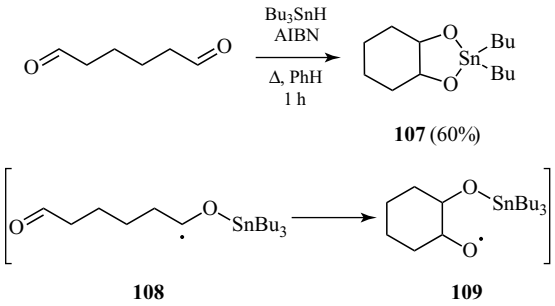

107 (60%)

108 **109**

Scheme 37 The stannacycle intermediate can sometimes be isolated.

monoxide the yield of this product was observed to increase to 65%.

The authors also explored the generality of 1,4-stannyl radical migrations (Scheme 34). Aromatic bromides (**101**) were reacted with *n*-tributyltin hydride under standard radical conditions resulting in the formation of the arylstannanes (**102**) as the only isolated products in good yields; these reactions presumably proceed through the intermediacy of radicals **103** and **104**.

There are now numerous examples of 1,*n*-translocation chemistry involving silicon, with a chiral example used to explore the stereochemical requirements of this homolytic substitution process (Scheme 5).[11] The majority of these reactions involve 1,2-migrations and include the radical Brook rearrangement, but there are reports of 1,3-, 1,4-, and 1,5-silyl migrations as well. Some illustrative examples of this chemistry are depicted in Scheme 35.[66–68]

5.2 Homolytic Substitution at Germanium and Tin

Intramolecular homolytic substitution reactions that afford germanium- or tin-containing heterocycles are very rare; indeed, to the best of our knowledge, there are no examples of this chemistry involving germanium; however, Fu and Hays reported stannane-mediated intramolecular pinacol-coupling reactions than involve the formation of stannacycles.[69] As shown in Scheme 36,

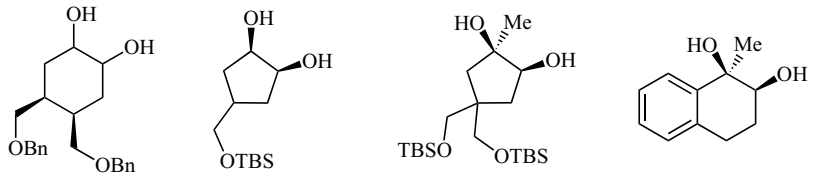

110 (88%) 1:1.6 **111** (64%) 99:1 **112** (62%) 20:1 **113** (53%) 20:1

Figure 8 Examples of products from stannane-mediated pinacol-coupling reactions.

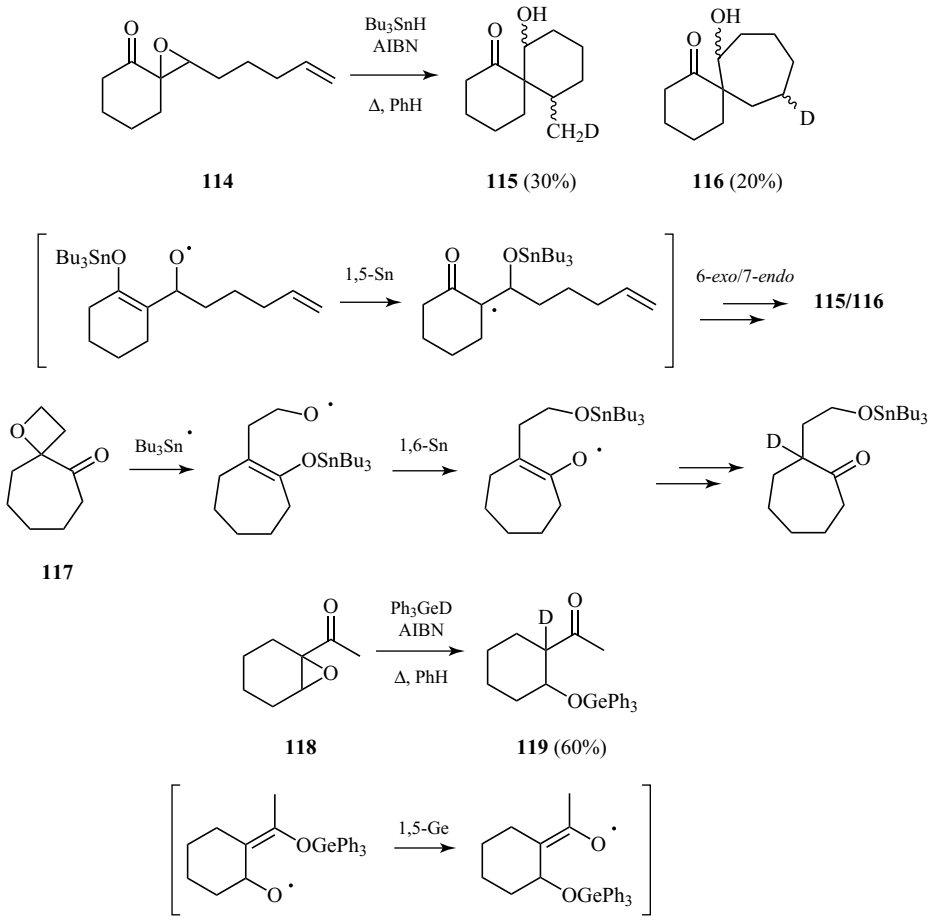

Scheme 38 Examples of homolytic 1,*n*-stannyl and germyl group translocations.

when glutaraldehyde (**104**) was reacted with *n*-tributyltin hydride under standard radical conditions, the cyclopentane-1,2-diol (**105**) could be isolated in 46% yield as a 98 : 1 ratio of cis : trans isomers, after aqueous work up. The authors postulate the involvement of stannacycle (**106**), formed by intramolecular homolytic substitution at tin, which was hydrolyzed to the diol upon aqueous work up.

In support of this hypothesis, the analogous 1,3-dioxa-2-stannolane **107** could be isolated in 60% yield from the corresponding reaction of adipaldehyde with *n*-tributyltin hydride, but required omission of the final hydrolysis step in

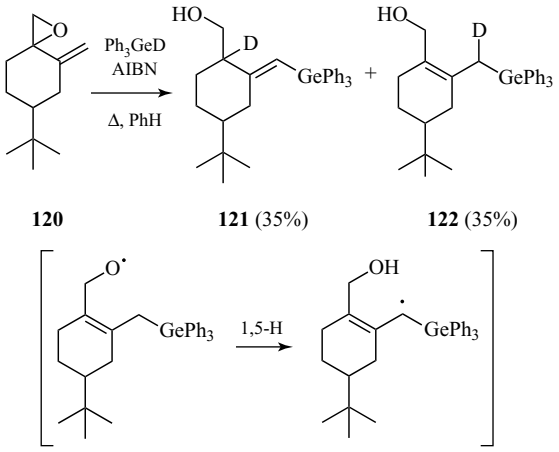

Scheme 39 1,5-Hydrogen transfer sometimes competes with germyl group translocation.

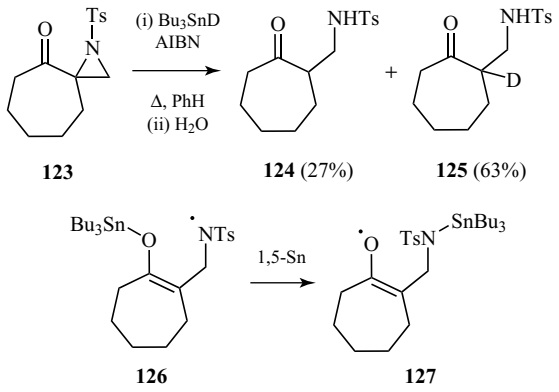

Scheme 40 Example of a 1,5-stannyl group translocation from oxygen to nitrogen.

the overall sequence.[69] Presumably, addition of the *n*-tributylstannyl radical to one of the aldehydes generates the radical **108** that cyclizes in a 6-exo manner onto the remaining aldehyde to afford the alkoxyl radical **109**. The mechanistic sequence is completed when cyclization of **109** at tin provides the 1,3-dioxa-2-stannolane **107** and a chain-carrying *n*-tributyltin radical (Scheme 37).

A variety of pinacol-coupling products were successfully prepared using this methodology, with 1,5-dicarbonyl substrates exhibiting high diastereoselectivity for the corresponding cis diol. For example, the diol **110** was obtained in good yield (88%) but with poor stereoselectivity (1 : 1.6 ratio cis : trans) while **111** was obtained as a 99 : 1 mixture

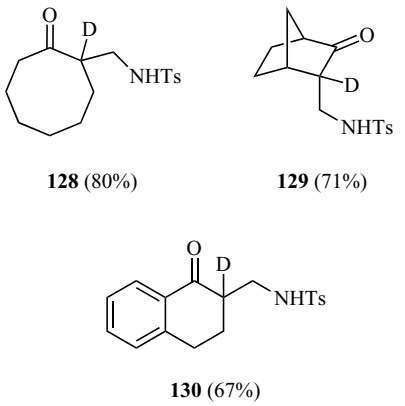

Figure 9 Some products from intramolecular homolytic transfers from oxygen to nitrogen.

of cis : trans isomers, but in lower yield. Cyclization of ketones was also possible, but in moderate yields; for example, **112** and **113** were isolated in 62 and 53% yields, respectively and in identical (20 : 1) cis : trans ratio (Figure 8).

There are several reported examples of 1,*n*-germyl and stannyl radical translocation reactions, and the majority of these are discussed in the 1996 review.[2] However, some examples are included in this article for completeness (Scheme 38). Treatment of epoxide (**114**) with *n*-tributyltin deuteride under standard radical conditions afforded the spiro-fused bicycles (**115, 116**) in moderate yield in a process that involves a 1,5-translocation of the *n*-tributylstannyl radical between oxygen centers, followed by either 6-exo-trig or 7-endo-trig ring closures.[70] Similar chemistry involving the oxetane (**117**) resulted in the analogous 1,6-translocation of the tin substituent,[70] while treatment of epoxide (**118**) with triphenylgermanium hydride resulted in a 60% yield of the germyl ether (**119**).[71]

It is important to note that, as observed in homolytic substitution chemistry involving sulfur, if there are abstractable hydrogen atoms available, 1,*n*-hydrogen atom transfer will compete with homolytic substitution at the less reactive elements (Si, Ge) as illustrated (Scheme 39) in the conversion of epoxide (**120**) to the germanes (**121, 122**).[71]

During the past decade, Kim and coworkers reported a 1,5-translocation of a stannyl radical from oxygen to nitrogen.[72] As shown in Scheme 40, the aziridine (**123**), when reacted with *n*-tributyltin deuteride under standard radical conditions afforded

ketones **124** and **125** in 90% overall yield, after aqueous work up. Deuterium labeling allowed the product (**126**) obtained from homolytic translocation of the tin-containing group at stannane to be distinguished from the product of direct reduction (**127**).

Presumably, the *n*-tributylstannyl radical adds to the ketone with subsequent or concerted rapid ring opening of the aziridine to give the nitrogen-centered radical **126**; direct reduction of **126** gives **124**. Alternatively **126** can undergo a 1,5-translocation to give **127**, which ultimately leads to ketone **125** (Scheme 40).

A number of other aziridines displayed similar reactivity providing the products (**128–130**) of translocation in good overall yield after hydrolysis (Figure 9).[72]

6 CONCLUSION

Intramolecular homolytic substitution chemistry offers the synthetic practitioner efficient and convenient methods for the preparation of higher heterocycles that complement existing ionic processes, especially for the preparation of ring systems containing sulfur and selenium, as well as silicon. As was observed during the free radical "renaissance period,"[73] important discoveries made in the field of intramolecular homolytic addition chemistry led to an appreciation of the factors that control carbon–carbon bond forming chemistry and this information revolutionized the acceptance of radical chemistry in synthesis. Similar key studies have led to an understanding of the factors that control homolytic substitution chemistry. There are now numerous examples of radical ring-closure reactions at sulfur, selenium, silicon and fewer examples involving tellurium and tin. It is particularly rewarding to see this chemistry being applied to molecules of biological significance that include potential next-generation antihypertensive drugs. We look forward to this chemistry developing further through exciting discoveries that are just around the corner.

REFERENCES

1. B. Giese, *Radicals in Organic Synthesis: Formation of Carbon–Carbon Bonds*, Pergamon Press, Oxford, 1986.
2. C. H. Schiesser and L. M. Wild, *Tetrahedron*, 1996, **52**, 13265–13314.
3. C. H. Schiesser, *Chem. Commun.*, 2006, 4055–4065.
4. J. C. Walton, *Acc. Chem. Res.*, 1998, **31**, 99–107.
5. D. Crich, *Helv. Chim. Acta*, 2006, **89**, 2167–2181.
6. S. E. Vaillard, C. Mück-Lichtenfeld, S. Grimme, and A. Studer, *Angew. Chem. Int. Ed.*, 2007, **46**, 6533–6536, references cited therein.
7. C. H. Schiesser and L. M. Wild, *J. Org. Chem.*, 1998, **63**, 670–676.
8. C. H. Schiesser and L. M. Wild, *J. Org. Chem.*, 1999, **64**, 1131–1139.
9. S. M. Horvat, C. H. Schiesser, and L. M. Wild, *Organometallics*, 2000, **19**, 1239–1246.
10. S. M. Horvat, S. Kim, and C. H. Schiesser, *Aust. J. Chem.*, 2002, **55**, 753–755.
11. S. M. Horvat, S. Kim, and C. H. Schiesser, *Chem. Commun.*, 2003, 1182–1183.
12. A. L. J. Beckwith and D. R. Boate, *J. Chem. Soc. Chem. Commun.*, 1986, 189–190.
13. H. Matsubara and C. H. Schiesser, *J. Org. Chem.*, 2003, **68**, 9299–9303.
14. A. L. J. Beckwith and S. A. M. Duggan, *J. Chem. Soc., Perkin Trans. 2*, 1994, 1509–1518.
15. J. A. Franz, D. H. Roberts, and K. F. Ferris, *J. Org. Chem.*, 1987, **52**, 2256–2262.
16. I. Ryu, T. Okuda, K. Nagahara, *et al*., *J. Org. Chem.*, 1997, **62**, 7550–7551.
17. S. Lobachevsky, C. H. Schiesser, C. Y. Lin, and M. L. Coote, *J. Phys. Chem. A*, 2008, **112**, 13622–13627.
18. S. Lobachevsky, PhD thesis, The University of Melbourne, Victoria, Australia, 2008.
19. L. M. Wild, PhD thesis, The University of Melbourne, Victoria, Australia, 1998.
20. J. E. Lyons, C. H. Schiesser, and K. Sutej, *J. Org. Chem.*, 1993, **58**, 5632–5638.
21. M. J. Laws and C. H. Schiesser, *Tetrahedron Lett.*, 1997, **38**, 8429–8432.
22. J. A. Kampmeier, R. B. Jordan, M. S. Liu, *et al*., in *Organic Free Radicals*, *ACS Symposium Series, No 69*, ed. W. A. Pryor, American Chemical Society, Washington, DC, 1978, pp. 275–289.
23. T. Ooi, M. Furuya, D. Sakai, and K. Maruoka, *Adv. Synth. Catal.*, 2001, **343**, 166–168.
24. J. Coulomb, V. Certal, L. Fensterbank, *et al*., *Angew. Chem. Int. Ed.*, 2006, **45**, 633–637.
25. J. Coulomb, V. Certal, M.-H. Larraufie, *et al*., *Chem.—Eur. J.*, 2009, **15**, 10255–10232.
26. S. H. Kyne, H. M. Aitken, C. H. Schiesser, *et al*., *Org. Biomol. Chem.*, 2011, **9**, 3331–3337.
27. D. Crich, T. K. Hutton, and K. Ranganathan, *J. Org. Chem.*, 2005, **70**, 7672–7678.
28. J. Malmström, M. Jonsson, I. A. Cotgreave, *et al*., *J. Am. Chem. Soc.*, 2001, **123**, 3434–3440.
29. S. Yolka, E. Dunach, M. Loiseau, *et al*., *Flavour Fragrance J.*, 2002, **17**, 425–431.
30. K. Sutej and C. H. Schiesser, *J. Chem. Soc., Chem. Commun.*, 1992, 57–58.
31. L. J. Benjamin, C. H. Schiesser, and K. Sutej, *Tetrahedron*, 1993, **49**, 2557–2566.
32. R. L. Grange, J. Ziogas, A. J. North, *et al*., *Biorg. Med. Chem. Lett.*, 2008, **18**, 1241–1244.
33. M. K. Staples and C. H. Schiesser, *Chem. Commun.*, 2010, **46**, 803–805.

34. M. K. Staples, R. L. Grange, J. A. Angus, *et al*., *Org. Biomol. Chem.*, 2011, **9**, 473–479.
35. M. C. Fong and C. H. Schiesser, *Tetrahedron Lett.*, 1993, **34**, 4347–4348.
36. M. A. Lucas and C. H. Schiesser, *J. Org. Chem.*, 1998, **63**, 3032–3036.
37. N. Al-Maharik, L. Engman, J. Malmström, and C. H. Schiesser, *J. Org. Chem.*, 2001, **66**, 6286–6290.
38. M. W. Carland, R. L. Martin, and C. H. Schiesser, *Org. Biomol. Chem.*, 2004, **2**, 2612–2618.
39. T. Fenner, J. M. White, and C. H. Schiesser, *Org. Biomol. Chem.*, 2006, **4**, 466–474.
40. L. Engman, M. J. Laws, J. Malmström, *et al*., *J. Org. Chem.*, 1999, **64**, 6764–6770.
41. D. Shanks, R. Amorati, M. G. Fumo, *et al*., *J. Org. Chem.*, 2006, **71**, 1033–1038.
42. T. Fenner and C. H. Schiesser, *Molecules*, 2004, **9**, 472–479.
43. M. W. Carland and C. H. Schiesser, *Molecules*, 2004, **9**, 466–471.
44. C. H. Schiesser and S.-L. Zheng, *Tetrahedron Lett.*, 1999, **40**, 5059–5062.
45. M. A. Lucas, O. T. K. Nguyen, C. H. Schiesser, and S.-L. Zheng, *Tetrahedron*, 2000, **56**, 3995–4000.
46. J. H. Byers and G. C. Lane, *J. Org. Chem.*, 1993, **58**, 3355–3360.
47. S. Lobachevsky, C. H. Schiesser, and V. Gupta, *Tetrahedron Lett.*, 2007, **48**, 9077–9079.
48. R. Leardini, G. F. Pedulli, A. Tundo, and G. Zanardi, *J. Chem. Soc., Chem. Commun.*, 1985, 1390–1391.
49. A. Ruwet and M. Renson, *Bull. Soc. Chim. Belg.*, 1970, **79**, 75–79.
50. A. Ruwet and M. Renson, *Bull. Soc. Chim. Belg.*, 1970, **79**, 593–599.
51. M. Degueil-Castaing, C. Navarro, F. Ramon, and B. Maillard, *Aust. J. Chem.*, 1995, **48**, 233–240.
52. G. F. Meijs, E. Rizzardo, and S. H. Thang, *Polym. Prepr.*, 1992, **33**, 893–894.
53. W. A. Nugent and T. V. Rajanbabu, *J. Am. Chem. Soc.*, 1988, **110**, 8561–8562.
54. T. V. Rajanbabu and W. A. Nugent, *J. Am. Chem. Soc.*, 1989, **111**, 4525–4527.
55. T. V. Rajanbabu, W. A. Nugent, and M. S. Beattie, *J. Am. Chem. Soc.*, 1990, **112**, 6408–6409.
56. T. V. Rajanbabu and W. A. Nugent, *J. Am. Chem. Soc.*, 1994, **116**, 986–997.
57. A. Gansäuer, B. Rinker, M. Pierobon, *et al*., *Angew. Chem. Int. Ed.*, 2003, **42**, 3687–3690.
58. A. Gansäuer, B. Rinker, N. Ndene-Schiffer, *et al*., *Eur. J. Org. Chem.*, 2004, 2337–2351.
59. A. Gansäuer, A. Fleckhaus, M. A. Lafont, *et al*., *J. Am. Chem. Soc.*, 2009, **131**, 16989–16999.
60. K. J. Kulicke, C. Chatgilialoglu, B. Kopping, and B. Giese, *Helv. Chim. Acta*, 1992, **75**, 935–939.
61. K. Miura, K. Oshima, and K. Utimoto, *Bull. Chem. Soc. Jpn.*, 1993, **66**, 2348–2355.
62. A. Studer, *Angew. Chem. Int. Ed.*, 1998, **37**, 462–465.
63. A. Studer and H. Steen, *Chem.—Eur. J.*, 1999, **5**, 759–773.
64. A. Blum, W. Hess, and A. Studer, *Synthesis*, 2004, 2226–2235.
65. A. Studer, S. Amrein, H. Matsubara, *et al*., *Chem. Commun.*, 2003, 1190–1191.
66. S. Shuto, M. Kanazaki, S. Ichikawa, and M. Matsuda, *J. Org. Chem.*, 1998, **63**, 746–754.
67. C. Chatgilialoglu, A. Guarini, A. Guerrini, and G. Seconi, *J. Org. Chem.*, 1992, **57**, 2207–2208.
68. S. Kim, J. Y. Do, and K. M. Lim, *J. Chem. Soc., Perkin Trans. 1*, 1994, 2517–2518.
69. D. S. Hays and G. C. Fu, *J. Org. Chem.*, 1998, **63**, 6375–6381.
70. S. Kim and K. M. Lim, *Tetrahedron Lett.*, 1993, **34**, 4851–4854.
71. S. Kim, J. Y. Do, and K. M. Lim, *Chem. Lett.*, 1996, 669–670.
72. S. Kim, M. S. Jung, C. H. Cho, and C. H. Schiesser, *Tetrahedron Lett.*, 2001, **42**, 943–945.
73. A. L. J. Beckwith and C. H. Schiesser, *Org. Biomol. Chem.*, 2011, **9**, 1736–1743.

Please note that the abstract and keywords will not be included in the printed book, but are required for the online presentation of this book which will be published on Wiley's own online publishing platform.

If the abstract and keywords are not present below, please take this opportunity to add them now. The abstract should be a short paragraph upto 200 words in length and keywords between 5 and 10 words.

Abstract: Intramolecular homolytic substitution chemistry offers the synthetic practitioner efficient and convenient methods for the preparation of higher heterocycles that complement existing ionic processes, especially for the preparation of ring systems containing sulfur and selenium, as well as silicon. This article details fundamental principles and important kinetic data for intramolecular homolytic substitution chemistry involving main group heteroatoms and provides examples and illustrative procedures for the application of this chemistry to the preparation of interesting molecules, some of which are of biological significance.

Keywords: homolytic substitution; intramolecular; sulfur; selenium; tellurium; silicon; germanium; tin; higher heterocycle.